http://dx.doi.org/10.5012/bkcs.2013.34.2.661

Thiadiazoloquinoxaline-Based Narrow Energy Gap Molecules for Small Molecule Solar Cell Applications

Vellaiappillai Tamilavan, Myungkwan Song,† Sung-Ho Jin,† and Myung Ho Hyun*

*Department of Chemistry and Chemistry Institute for Functional Materials, Pusan National University, Busan 690-735, Korea. *E-mail: mhhyun@pusan.ac.kr*
†Department of Chemistry Education and Interdisciplinary Program of Advanced Information and Display Materials, Pusan National University, Busan 609-735, Korea
Received October 30, 2012, Accepted November 22, 2012

Key Words : Bulk heterojunction solar cell, Organic solar cell, Organic small molecule, Low band gap molecule, Thiadiazoloquinoxaline

Polymer bulk heterojunction (BHJ) solar cells consisting of the photoactive layer containing the interpenetrating network of electron donating polymer and electron accepting $PC_{71}BM$ has been proved to be quite effective in converting the solar energy into electrical energy.[1] After many efforts, the power conversion efficiency (PCE) of the polymer solar cells (PSCs) was improved up to 9.2%.[1] Unfortunately, the PCEs of the PSCs were found to be highly affected by the synthetic characteristics of the donor polymers. At present, the poor reproducibility of the synthetic polymer characteristics such as purity, molecular weight, regioregularity and polydispersity of each batch of the polymerization limits the commercial application of PSCs.[2] On the other hand, small molecule organic solar cells (SMOSCs) fabricated from the photoactive layer containing organic small molecule as an electron donor and $PC_{71}BM$ as an electron acceptor also showed promising performances in terms of PCE.[3-8] The PCE of the solution-processed SMOSCs was reached up to 7%.[3] and that for the vacuum-processed tandem SMOSCs was improved up to 10.7%.[4] The overall PCE of SMOSCs is quite close to the maximum PCE obtained from the PSCs. This inspires us to develop new low band gap small molecules for SMOSCs application.

It is well known that the PCE of solar cell devices is strongly dependent on the light harvesting ability of the photoactive layer. To improve the light harvesting ability of the active layer, it is essential to utilize the donor molecules which can absorb the sun light from 300 nm to 1000 nm, along with that the absorption band of donor molecules should be located at the maximum solar flux region (500 nm to 800 nm) of the solar spectra. In our attempt to prepare narrow energy gap small molecules, we were interested in utilizing thiadiazoloquinoxaline units, because certain polymers containing thiadiazoloquinoxaline units have been known to show their absorption band from 300 nm to 1200 nm.[9,10] In this study, we prepared two new thiadiazoloquinoxaline-based low band gap small molecules, TDQ-SM1 and TDQ-SM2, shown in Scheme 1 and studied their optical, electrical and photovoltaic properties.

In this study, to recognize the influence of the substituent bonded to the quinoxaline ring of the thiadiazoloquinoxaline unit, isobutyl and thiophene substituted thiadiazoloquinoxaline compounds 1 and 2 were coupled with commercially available trans-2-(4-pentylphenyl)vinylboronic acid pinacol

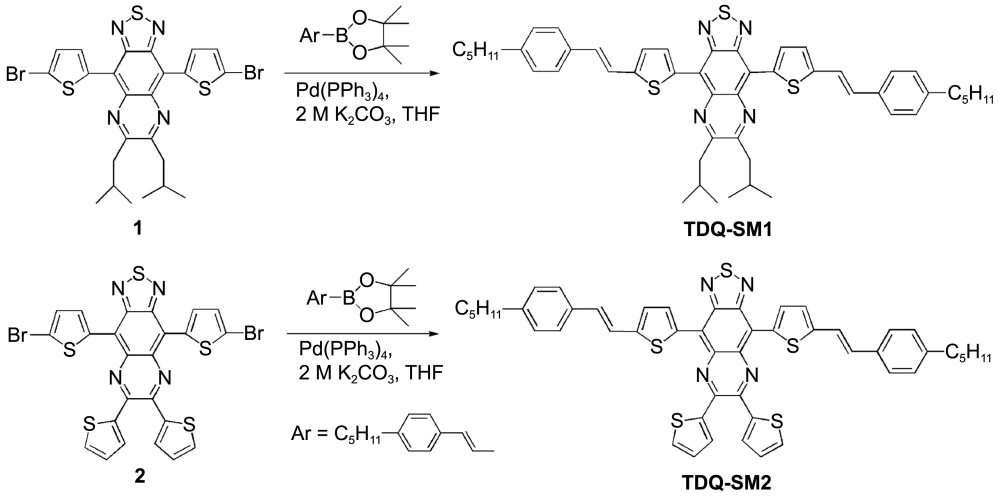

Scheme 1. Synthetic routes for TDQ-SM1 and TDQ-SM2.

ester to afford two new organic small molecules TDQ-SM1 and TDQ-SM2. The synthetic routes for the synthesis of TDQ-SM1 and TDQ-SM2 are outlined in Scheme 1. Compounds 1 and 2 were synthesized *via* the procedures reported.[9,10] The weak electron donating trans-2-(4-pentylphenyl)vinyl group used in this study is expected to increase the charge carrier mobility while maintaining the HOMO energy level of the final molecules. Usually, the incorporation of strong electron donor groups raises the HOMO energy level of the final molecules. However, the weak donor group might maintain the HOMO energy level. In addition, the high charge carrier mobility is expected due to the extended conjugation length[11] and the possibility for dense packing through the intermolecular van der Waals interactions between flexible alkyl groups and planar aromatic rings in neighboring molecular layers.[5,12] TDQ-SM1 exhibited excellent solubility in chloroform, and chlorobenzene, whereas molecule TDQ-SM2 showed good solubility in chlorobenzene and moderate solubility in chloroform at room temperature. TDQ-SM1 and TDQ-SM2 showed high thermal stability with the 5% weight loss temperature of 330 °C and 385 °C, respectively.

The absorption spectra of TDQ-SM1 and TDQ-SM2 were measured in chloroform (1.0×10^{-5} M) and as thin films (on glass) at room temperature (Fig. 1). TDQ-SM1 and TDQ-SM2 show two absorption bands in both solution and film state. The first absorption bands at the region of 300-500 nm are attributed to the π-π* electronic transition and the another absorption bands at the region of 500-900 nm for TDQ-SM1 and 500-1100 nm for TDQ-SM2 are originated from the donor-acceptor internal charge transfer.[9,10] TDQ-SM1 shows their absorption maxima at 397 nm (ε = 3.91 × 10^4) and 715 nm (ε = 2.07 × 10^4) in solution and at 390 nm and 692 nm in film state, whereas TDQ-SM2 shows their absorption maxima at 411 nm (ε = 5.90 × 10^4) and 775 nm (ε = 2.28 × 10^4) in solution and at 411 nm and 840 nm in film state. The film state absorption spectra of TDQ-SM1 and TDQ-SM2 were found to be quite much broader than the solution state absorption spectra, indicating that the molecules are well orientated in solid state than in the solution state. Interestingly, the optical properties of the thiadiazoloquinoxaline-based molecules were found to be highly influenced by the substituent on the quinoxaline ring. Simply by changing the substitution from isobutyl (TDQ-SM1) to thiophene (TDQ-SM2) on the quinoxaline ring of the thiadiazoloquinoxaline unit, the absorption onset was shifted from 900 nm to 1100 nm in film state. In addition, the absorption band was also found to be quite broad at the low energy part of the solar spectrum. The optical band gap ($E_{g,opt}$) of TDQ-SM1 and TDQ-SM2 was calculated from the onset wavelength of the optical absorption as thin film to be 1.36 eV and 1.15 eV, respectively. The optical properties of TDQ-SM1 and TDQ-SM2 are summarized in Table 1.

The onset oxidation ($E_{ox,onset}$) and reduction ($E_{red,onset}$) potential of TDQ-SM1 and TDQ-SM2 were estimated from cyclic voltammetry (CV) analysis. The CV spectra of TDQ-SM1 and TDQ-SM2 are presented in Figure 2. The HOMO and LUMO energy levels of TDQ-SM1 and TDQ-SM2 were calculated to be −5.26 eV, −5.22 eV and −3.86 eV, −3.97 eV, respectively. The electrochemical band gaps ($E_{g,elc}$) of TDQ-SM1 and TDQ-SM2 were determined from the HOMO and LUMO energy levels to be 1.40 eV and 1.25 eV, respec-

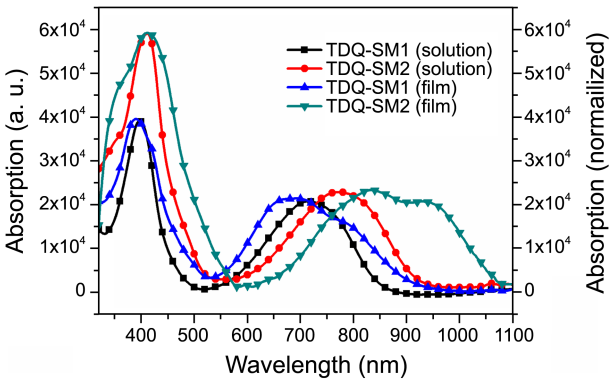

Figure 1. Absorption spectra of TDQ-SM1 and TDQ-SM2 in chloroform (1×10^{-5} M) and thin film on glass (normalized).

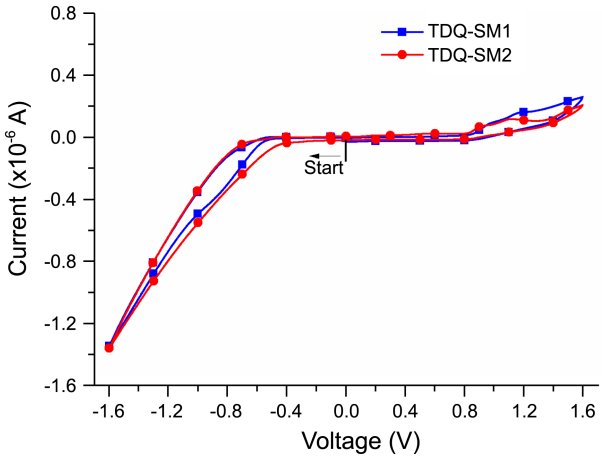

Figure 2. Cyclic voltammogram of TDQ-SM1 and TDQ-SM2 in chloroform (1×10^{-4} M).

Table 1. Summary of the optical, electrochemical and photovoltaic properties of TDQ-SM1 and TDQ-SM2

Molecule	λ_{max} in solution (nm)[a]	λ_{max} film (nm)[b]	$E_{g,opt}$ (eV)[c]	HOMO (eV)[d]	LUMO (eV)[d]	$E_{g,elc}$ (eV)[d]	V_{oc} (V)[e]	J_{sc} (mA/cm^2)[f]	*FF* (%)[g]	*PCE* (%)[h]
TDQ-SM1	397, 715	390, 692	1.36	−5.26	−3.86	1.40	0.42	2.42	24	0.24
TDQ-SM2	411, 775	411, 840	1.15	−5.22	−3.97	1.25	0.38	1.40	26	0.14

[a]Absorption maximum of the molecules in chloroform solution. [b]Absorption maximum of the molecules as thin film onto the glass substrate. [c]The optical band gap estimated from the onset wavelength of the optical absorption in thin film. [d]The HOMO, LUMO and electrochemical band gap of the molecules estimated from cyclic voltammetry analysis. [e]Open-circuit voltage. [f]Short-circuit current density. [g]Fill factor. [h]Power conversion efficiency.

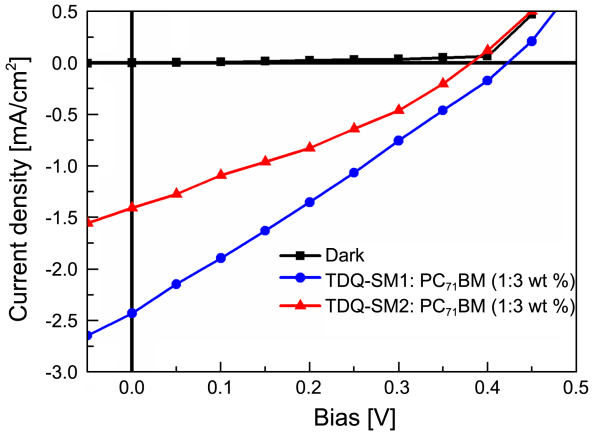

Figure 3. *J-V* characteristics of ITO/PEDOT:PSS/TDQ-SM1 or TDQ-SM2:$PC_{71}BM$ (1:3 wt %)/TiO_x/Al devices.

tively. The optical and electrochemical band gap values are correlated well with each other. The incorporation of thiophene instead of isobutyl on the quinoxaline ring of the thiadiazoloquinoxaline unit slightly raised the HOMO energy level of the final molecule. In addition, the LUMO energy level was notably lowered. The electrochemical properties of TDQ-SM1 and TDQ-SM2 are summarized in Table 1.

The SMOSCs were fabricated with the device structure of ITO/PEDOT:PSS/TDQ-SM1 or TDQ-SM2:$PC_{71}BM$ (1:3 wt %)/TiO_x/Al. The current density-voltage (*J-V*) characteristic curve of the SMOSC devices measured under the AM 1.5 G irradiation (100 mWcm^{-2}) are shown in Figure 3 and the data are summarized in Table 1. The device fabricated from TDQ-SM1:$PC_{71}BM$ (1:3 wt %) as the active layer shows the PCE of 0.24% with a J_{sc} of 2.42 mA/cm^2, a V_{oc} of 0.42 V, and a *FF* of 24% while that fabricated from TDQ-SM1:$PC_{71}BM$ (1:3 wt %) as the active layer shows the PCE of 0.14% with a J_{sc} of 1.40 mA/cm^2, a V_{oc} of 0.38 V, and an *FF* of 26%. The overall photovoltaic performance was found to be better for TDQ-SM1 based SMOSC device even though the absorption of TDQ-SM2 was quite broad up to 1100 nm. For the efficient charge separation at donor-acceptor interface, the energy difference between the LUMO level of donor and LUMO level of acceptor should be over 0.2-0.3 eV.[13] However, the LUMO energy level of TDQ-SM2 is very close to the LUMO level of $PC_{71}BM$. Consequently, the charge separation in the TDQ- SM2:$PC_{71}BM$ active layer is expected to be reduced and the PCE of the device made from TDQ-SM2:$PC_{71}BM$ is expected to be lower than that of the device made from TDQ-SM1:$PC_{71}BM$.

The morphology of active layers plays an important role in the device performance.[14] To evaluate the blending nature of the active layer of SMOSCs, the surface of the ITO/PEDOT:PSS/TDQ-SM1 or TDQ-SM2:$PC_{71}BM$ (1:3 wt %) substrates was investigated by using atomic force microscope (AFM) analysis. The AFM images are shown in Figure 4. The root-mean-square (rms) roughness of the active layers was found to be 0.53 nm and 1.75 nm, respectively. The relatively smoother surface and better blending nature of the TDQ-SM1:$PC_{71}BM$ (1:3 wt %) active layer might be also responsible for the better photovoltaic performance of TDQ-SM1 based SMOSCs.

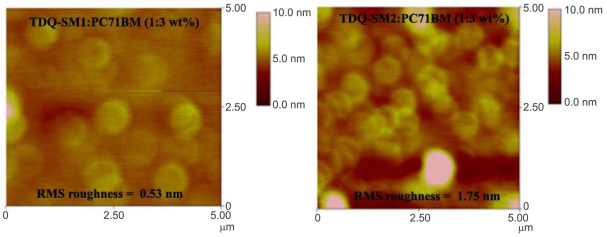

Figure 4. AFM image of ITO/PEDOT:PSS/TDQ-SM1 or TDQ-SM2:$PC_{71}BM$ (1:3 wt %) substrates.

In summary, two new thiadiazoloquinoxaline-based small molecules, TDQ-SM1 and TDQ-SM2, were prepared. Relatively more extended π-conjugated molecule, TDQ-SM2, was found to show broader and red shifted absorption band compared to that of TDQ-SM1. The optical band gap of TDQ-SM1 and TDQ-SM2 was calculated to be 1.36 eV and 1.15 eV, respectively, indicating that changing the substituent on the quinoxaline ring of the thiadiazoloquinoxaline unit from isobutyl to thiophene significantly compress the HOMO-LUMO energy level of the molecule. The solution processed SMOSC devices prepared by using the configuration of ITO/PEDOT:PSS/TDQ-SM1 or TDQ-SM2:$PC_{71}BM$ (1:3 wt %)/TiO_x/Al showed maximum PCEs of 0.24% and 0.14%, respectively. The absorption band of TDQ-SM1 appearing exactly at the maximum solar flux region, relatively smooth active layer surface and the better charge separation at donor-acceptor interface are expected to be the reason for the better photovoltaic performance of the device made from TDQ-SM1. Our findings suggest that the substituent on the quinoxaline ring of the thiadiazoloquinoxaline unit highly influences the optical, electrical and photovoltaic properties of the final molecules. We believe that these results are helpful in deigning new broad absorption molecules for solar cell applications.

Experimental

Materials and Instruments. All reagents were commercially available from Aldrich chemicals and used without further purification. ^{1}H and ^{13}C NMR spectra were recorded with a 300 and 75 MHz Varian Mercury Plus spectrometer in deuterated chloroform. Melting point was determined by using Gallenkamp Variable Heater. The TGA (Mettler Toledo TGA/SDTA 851) and DSC (SETARAM instrumentation analyzer) analyses were performed under a nitrogen atmosphere at a heating rate of 10 °C/min. Infrared spectra were obtained on a Nicolet 380 FTIR spectrophotometer with samples prepared as KBr pellets. The absorption spectra were recorded with a JASCO V-570 spectrophotometer. The electrochemical property of the polymer was studied with a CH Instruments Electrochemical Analyzer. The SMOSC device performance was measured using a AM 1.5G solar simulator (Oriel 300 W) at 100 mWcm^{-2} light illumination.

Current-voltage (*J-V*) characteristics of the photovoltaic cell were measured using a standard source measurement unit (Keithley 236). The thickness of the thin films was measured using a KLA Tencor Alpha-step IQ surface profilometer with an accuracy of ± 1 nm. Atomic force microscopy (AFM) images of blend films were obtained on a Veeco-Multimode AFM operating in the tapping mode.

Synthesis of 4,9-bis(5-(4-Hexylstyryl)thiophen-2-yl)-6,7-diisobutyl-[1,2,5]thiadiazolo[3,4-*g*]quinoxaline (TDQ-SM1). The stirred solution of compound **1**, 4,9-bis(5-bromothiophen-2-yl)-6,7-diisobutyl-[1,2,5]thiadiazolo[3,4-*g*]quinoxaline, (0.31 g, 0.5 mmol) and trans-2-(4-pentylphenyl)vinylboronic acid pinacol ester (0.36 g, 1.2 mmol) in THF (60 mL) was purged well with nitrogen for 45 min. Subsequently, $Pd(PPh_3)_4$ (0.05 g, 8 mol %) and aqueous 2 M K_2CO_3 (7 mL) were added and the mixture was refluxed with vigorous stirring for 24 h under nitrogen atmosphere. The reaction mixture was cooled to room temperature and concentrated by rotary evaporation. The residue was dissolved into 50 mL of CH_2Cl_2 and washed with 2 N HCl (50 mL) and then with brine (50 mL). The organic layer was dried over anhydrous $NaSO_4$, filtered, evaporated on a rotary evaporator to dryness, and the residue was purified by column chromatography (hexane:ethyl acetate, 7:3 v/v) to afford TDQ-SM1. Yield 0.33 g (83%). mp 203-204 °C; ^{1}H NMR (300 MHz, $CDCl_3$) δ 8.98 (d, 2 H), 7.44 (d, 4 H), 7.06-7.34 (m, 10 H), 3.05 (d, 4 H), 2.66-2.80 (m, 2 H), 2.62 (t, 4 H), 1.60-1.70 (m, 4 H), 1.28-1.40 (m, 8 H), 1.17 (d, 12 H), 0.91 (t, 6 H); ^{13}C NMR (75 MHz, $CDCl_3$) δ 156.5, 151.6, 148.0, 143.1, 135.5, 135.2, 134.9, 134.1, 129.3, 129.1, 126.6, 126.3, 121.7, 120.6, 44.4, 36.0, 31.7, 31.3, 28.1, 23.4, 22.8, 14.3; IR (KBr, cm^{-1}): 3016, 2954, 2925, 2856, 1433; HRMS (EI^+, *m/z*) [m^+] Calcd for $C_{50}H_{56}N_4S_3$ 808.3667, found 808.3671.

Synthesis of 4,9-bis(5-(4-Hexylstyryl)thiophen-2-yl)-6,7-di(thiophen-2-yl)-[1,2,5]thiadiazolo[3,4-*g*]quinoxaline (TDQ-SM2). TDQ-SM2 was prepared *via* the identical procedure for the preparation of TDQ-SM1 except that compound **2**, 4,9-bis(5-bromothiophen-2-yl)-6,7-di(thiophen-2-yl)-1,2,5] thiadiazolo[3,4-*g*]quinoxaline, (0.34 g, 0.5 mmol) was taken instead of compound **1**. Yield 0.35 g (81%). mp 254-255 °C; ^{1}H NMR (300 MHz, $CDCl_3$) δ 8.81 (d, 2 H), 7.63 (d, 2 H), 7.53 (d, 2 H), 7.43 (d, 4 H), 7.02-7.24 (m, 12 H), 2.63 (t, 4 H), 1.60-1.72 (m, 4 H), 1.30-1.44 (m, 8 H), 0.93 (t, 6 H); ^{13}C NMR (75 MHz, $CDCl_3$) δ 156.9, 152.0, 148.5, 145.5, 143.0, 141.8, 135.4, 134.9, 134.5, 134.2, 131.7, 130.8, 129.0, 127.7, 126.7, 126.5, 121.6, 120.6, 36.0, 31.8, 31.4, 22.8, 14.3; IR (KBr, cm^{-1}): 3016, 2953, 2923, 2852, 1412; HRMS (EI^+, *m/z*) [m^+] Calcd for $C_{50}H_{44}N_4S_5$ 860.2170, found 860.2173.

Acknowledgments. This research was supported by the New & Renewable Energy program of the Korea Institute of Energy Technology Evaluation and Planning (KETEP) grant (No. 20103020010050) funded by the Ministry of Knowledge Economy, Republic of Korea.

Supporting Information. The detailed SMOSC device fabrication, ^{1}H-NMR, ^{13}C-NMR, IR spectra and TGA, DSC curves of TDQ-SM1 and TDQ-SM2 were presented in supplementary.

References

1. He, Z.; Zhong, C.; Su, S.; Xu, M.; Wu, H.; Cao, Y. *Nat. Photon.* **2012**, *6*, 591.
2. Kim, J.; Cho, N.; Ko, H. M.; Kim, C.; Lee, J. W.; Ko, J. *Sol. Energ. Mat. Sol. C* **2012**, *102*, 159.
3. van der Poll, T. S.; Love, J. A.; Nguyen, T. Q.; Bazan, G. C. *Adv. Mater.* **2012**, *24*, 3646.
4. http://www.heliatek.com.
5. Fitzner, R.; Elschner, C.; Weil, M.; Uhrich, C.; Körner, C.; Riede, M.; Leo, K.; Pfeiffer, M.; Reinold, E.; Mena.-Osteritz, E.; Bauerle, P. *Adv. Mater.* **2012**, *24*, 675.
6. Chen, Y.-H.; Lin, L.-Y.; Lu, C-W.; Lin, F.; Huang, Z.-Y.; Lin, H.-W.; Wang, P.-H.; Liu, Y.-H.; Wong, K.-T.; Wen, J.; Miller, D. J.; Darling, S. B. *J. Am. Chem. Soc.* **2012**, *134*, 13616.
7. Mishra, A.; Bauerl, P. *Angew. Chem. Int. Ed.* **2012**, *51*, 2020.
8. Sun, Y.; Welch, G. C.; Leong, W. L.; Takacs, C. J.; Bazan, G. C.; Heeger, A. *J. Nat. Mater.* **2012**, *11*, 44.
9. Tamilavan, V.; Song, M.; Jin, S.-H.; Hyun, M. H. *Synthetic Met.* **2011**, *161*, 1199.
10. Tamilavan, V.; Song, M.; Jin, S.-H.; Park, H. J.; Yoon, U. C.; Hyun, M. H. *Synthetic Met.* **2012**, *162*, 1184.
11. Schilinsky, P.; Asawapirom, U.; Scherf, U.; Biele, M.; Brabec, C. *J. Chem. Mater.* **2005**, *17*, 2175.
12. Meng, H.; Sun, F.; Goldfinger, M. B.; Gao, F.; Londono, D. J.; Marshal, W. J.; Blackman, G. S.; Dobbs, K. D.; Keys D. E. *J. Am. Chem. Soc.* **2006**, *128*, 9304.
13. Zhu, Z.; Waller, D.; Gaudiana, R.; Morana, M.; Mu1hlbacher, D.; Scharber, M.; Brabec, C. *Macromolecules* **2007**, *40*, 1981.
14. Kastner, C.; Susarova, D. K.; Jadhav, R.; Ulbricht, C.; Egbe, D. A. M.; Rathgeber, S.; Troshinb, P. A.; Hoppe, J. *Mater. Chem.* **2012**, *22*, 15987.